

ChemComm

Accepted Manuscript



This is an *Accepted Manuscript*, which has been through the Royal Society of Chemistry peer review process and has been accepted for publication.

Accepted Manuscripts are published online shortly after acceptance, before technical editing, formatting and proof reading. Using this free service, authors can make their results available to the community, in citable form, before we publish the edited article. We will replace this *Accepted Manuscript* with the edited and formatted *Advance Article* as soon as it is available.

You can find more information about *Accepted Manuscripts* in the [Information for Authors](#).

Please note that technical editing may introduce minor changes to the text and/or graphics, which may alter content. The journal's standard [Terms & Conditions](#) and the [Ethical guidelines](#) still apply. In no event shall the Royal Society of Chemistry be held responsible for any errors or omissions in this *Accepted Manuscript* or any consequences arising from the use of any information it contains.

Immobilization of isolated FI catalyst on polyhedral oligomeric silsesquioxane-functionalized silica for the synthesis of weakly entangled polyethylene

Received 00th January 20xx,
Accepted 00th January 20xx

DOI: 10.1039/x0xx00000x

Wei Li,^{*a} Huaqin Yang,^a Jingjing Zhang,^a Jingshan Mu,^a Dirong Gong^a and Xiaodong Wang^b

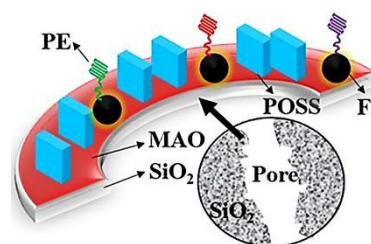
www.rsc.org/

Polyhedral oligomeric silsesquioxanes (POSSs) were adsorbed on methylaluminoxane-activated silica for the immobilization of fluorinated bis(phenoxyimine)Ti complexes (FI catalyst). These POSSs have been characterized as horizontal spacers isolating the active sites and hindering the chain overlap in polymerization. The heterogeneous catalyst exhibits considerable activity in the synthesis of weakly entangled polyethylene.

Entanglement density is a critical characteristic largely determining the melt visco-elasticity and crystalline order of polymers.¹ High entanglement density, which usually results from intertwined chains failing to unravel during crystal formation, can significantly decrease the crystalline order and processability of polymers.² It is therefore desirable to access nascent polymer with weakly entangled state in order to improve its processability, thermal and mechanical properties.³⁻⁵ This becomes crucial for the ultra-high molecular weight polyethylene (UHMWPE) due to its extremely high molten viscosity.³

To synthesize weakly entangled polyethylene (PE), it is necessary to establish a polymerization environment where the chain crystallization rate is faster than that of the chain propagation and also the chain overlap behaviour is prevented during polymerization. To this aim, low reaction temperature (*e.g.*, ≤ 30 °C)³⁻⁵ is important for achieving the former and the isolation of active sites (*e.g.*, by dilution³ or compartmented space^{4,5}) is essential for the latter. For instance, Rastogi *et al.*^{3a,d} synthesized a weakly entangled UHMWPE using diluted fluorinated bis(phenoxyimine)Ti complexes (FI catalyst) at room temperatures (≤ 30 °C). A dilute FI concentration separated the active sites to an extent that the growing chains did not meet each other, in favour of the hindrance of chain overlap. The nascent polymers presented a great improvement in processability (processed even in solid state) and tensile

strength.^{3b} Catalyst immobilization (*i.e.*, heterogeneous catalyst) exhibits a great potential of being transferred to industrial continuous processes due to the ease of preparation, separation and handling, where the catalyst particles can help direct the morphology of polymers and prevent reactor fouling.⁶ However, the active sites are tethered on a support and are usually close to each other, leading to a higher probability of chain overlap and the formation of entanglements during polymerization.^{3d} POSS, whose typical bulk cage consists of 8-10 Si atoms (diameter = ~ 3 -8 nm, excluding the periphery),⁷ can be utilized as a spacer to separate active sites. Santos *et al.* reported metallocene immobilization on the silica modified by a POSS with β -hydroxytertiary amine groups that also accommodated metallocene (in addition to the surface SiOH groups).⁸ However, it was reported that the onset of chain folding was from 65 to 150 carbon atoms (ranging from 8.5 nm-19.3 nm) for solution-crystallized linear *n*-alkanes.⁹ Thus, the close distance between those anchored points of active sites (*i.e.*, multi-functional groups of POSS and the adjacent -OH of silica) failed to separate the growing PE chains sufficiently.⁸



Scheme 1 Immobilized FI catalyst on POSS modified silica.

With the explicit aim to produce weakly entangled PE using a heterogeneous catalyst, we have for the first time employed a POSS consisting of only two -OH groups (incompletely condensed silsesquioxane) to functionalize silica (pre-modified chemically by a layer of methylaluminoxane (MAO)) for the immobilization of FI catalyst (see Fig. S1 in the ESI for the structures of POSS and FI). Our proposed method is that after the consumption of -OH groups (bonded to Al atoms), POSS

^a Department of Polymer Science and Engineering, School of Material Science and Chemical Engineering, Ningbo University, Ningbo, 315211, Zhejiang, P. R. China. Email: liwei@nbu.edu.cn

^b School of Engineering, University of Aberdeen, Aberdeen AB24 3UE, Scotland, United Kingdom.

Electronic Supplementary Information (ESI) available: General experimental details and the characterization of POSS-functionalized silica, immobilized FI catalysts and polymer products. See DOI: 10.1039/x0xx00000x

exhibits no extra site for FI and its steric hindrance effect thus serves to (i) block nearby Al sites enlarging the distance between the immobilized FI and (ii) separate the growing polymer chains (Scheme 1). We report here the preliminary results using ethylene polymerization as a representative reaction.

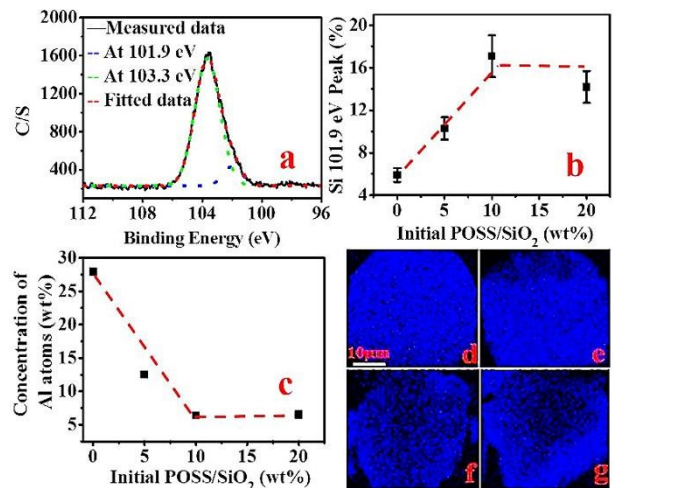


Fig. 1 Element analysis of the POSS/SiO₂ supports. (a) XPS spectra over the Si 2*p* region for POSS/SiO₂-10; (b) Percentage of Si 2*p* as a function of POSS loading on silica measured by XPS; (c) Concentration of Al atoms on the surface of POSS/SiO₂ measured by EDX; and (d-g) Distribution of Al atoms on the surface of POSS/SiO₂ measured by EDX (POSS loading (wt%): (d) 0, (e) 5, (f) 10 and (g) 20).

The morphology of POSS/SiO₂ supports shows similar spherical structure with a diameter around 30-50 μm (see Fig. S2 in the ESI), the clean surface (*i.e.*, no aggregator or fragment with small size) of which indicate that there is no noticeable residual POSS over the prepared supports, *i.e.*, effective POSS deposition. The surface Si element is examined by XPS analysis (see Fig. 1) to check POSS adsorption with typical XPS spectra given in Fig. S3. The Si 2*p* spectrum presents two signals at 103.3 and 101.9 eV (see Fig. 1a) that can be attributed to the contributions of Si atoms in the bulk and at the external surface, respectively.⁸ The amount of surface Si (2*p* at 101.9 eV) increased almost linearly with increasing nominal POSS/SiO₂ loading to 10 wt% and then became stable (see Fig. 1b). The ultimate POSS loadings determined by XPS analysis match well with the nominal ones (*i.e.*, 3.5 vs. 5.0 wt% and 8.7 vs. 10.0 wt%) except that only 8.6 wt% was obtained for the 20 wt% case (see Table S1 in the ESI). This presents a first indication of surface saturation by POSS at high loading. The binding energy (BE) of Al 2*p* around 74.1 eV increases with increasing POSS loading also to 10 wt% (See Table S2 in the ESI), suggesting the presence of electron deficient Al atoms as a result of the chemical bonding between MAO and -OH groups of POSS.¹⁰ This is consistent with spectroscopic evidence in the literature which has established that POSS was adsorbed by covalent bonds with the support surface at higher concentrations (> 1 wt%).^{8b} However, no more covalent bonds were formed with the excessive POSS

feed (*e.g.*, 20 wt%). The amount and distribution of Al elements on the surface of POSS/SiO₂ supports are shown in Fig. 1c,d-g, respectively. The amount of Al decreases nearly linearly to a minimum when the fraction of POSS is increased from 0 to 10 wt%, with no further change with POSS content. These results indicate that the MAO modified silica surface has been saturated by POSS at a loading of 10 wt%. Moreover, the MAO layer is covered by the adsorbed large POSS molecules, which affect the visibility of Al atoms by EDX. This is in line with our hypothesis that the steric hindrance effect of POSS may block adjacent Al atoms from being accessed. These POSSs exhibit a uniformed distribution on the silica surface notably at the saturation loading (Fig. 1f). The above characterization results demonstrate that the POSS has been evenly deposited on the MAO modified silica with surface saturation at a 10 wt% loading.

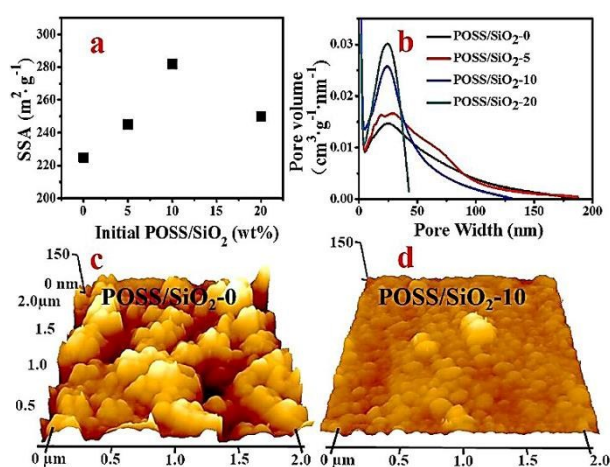


Fig. 2 (a) SSA and (b) pore size distribution of the POSS/SiO₂ supports. Surface imaging measured by scanning probe microscope (SPM) (c) POSS/SiO₂-0 and (d) POSS/SiO₂-10. The support is named as POSS/SiO₂-X where X (= 0, 5, 10 and 20) represents the nominal loading of POSS/SiO₂.

Fig. 2 presents the specific surface area (SSA) and pore size distribution of the POSS/SiO₂ supports, where detailed adsorption and desorption isotherms are available in Fig. S4. The SSA increased with the nominal loading of POSS/SiO₂ up to 10 wt% (see Fig. 2a) and then declined with a further increase in POSS loading. The immobilization of POSS into silica can increase the tortuosity of the pores resulted in a higher SSA.¹¹ The fraction of pores with large size decreases gradually while more pores with small size are evident with increasing POSS (see Fig. 2b). This indicates that POSS can adsorb effectively on the silica surface, especially on the surface of pores with a large size (with easy diffusion). It is noteworthy that when POSS was supplied in excess (*i.e.*, 20 wt%), it indeed not only decreases the pore size (adsorbed in large pores) but also obstructs some pores (accumulated POSSs in pore channels). This led to a decrease in both the SSA and the pore size (see Fig. 2a,b). This can be further evidenced by the surface imaging (Fig. 2c,d) detected by SPM where the surface of silica can be covered by small particles with a size of 50-100 nm, leading to a smoother surface than the POSS-free support.

The ultimate loadings of FI over the POSS/SiO₂ supports (determined by ICP analysis using Ti atoms) are close to 1 wt% with only FI/POSS/SiO₂-20 lower than this (see Table 1). The lack of large pores in POSS/SiO₂-20 (see Fig. 2) are unfavourable for FI diffusing into the pores as well as subsequently bond formation. The XPS spectra of the immobilized FI catalysts (taking FI/POSS/SiO₂-10 as a representative) are given in Fig. 3a,b and Fig. S5 where the BE of Ti 2*p* and Al 2*p* are summarized in Table S2. The BE of Ti 2*p*_{3/2} and Ti 2*p*_{1/2} of the homogenous FI catalyst have been characterized at 455.7 and 461.7 eV, respectively.^{12a} In this work, they increase to 456.7 and 462.7 eV after immobilization on POSS/SiO₂-0, demonstrating a decrease in Ti electron density, a result of electron transfer from Ti to MAO.^{12a,b} The BE of Ti 2*p* has been identical for all the samples with no more than 10 wt% of POSS, suggesting that the immobilized mechanism of FI has not been changed. However, a further increase in Ti 2*p* BE to 457.1 and 463.2 eV was observed for FI/POSS/SiO₂-20 (Table S2). This can be linked to the free Si-OH bonds of excessive POSS (those unreacted with MAO and physically attached/accumulated in the channels leading to pore blockage, see Fig. 1g and 2b) through which Si-O-Ti bonds can be formed, further decreasing the electron density of Ti. A similar response has been noticed in the literature where physically adsorbed superfluous POSS can provide extra sites for metallocene with a consequent increase in Zr 2*p* BE values.^{8,12c} The BE of Al 2*p* in the FI/POSS/SiO₂ catalysts decreases considerably compared with that of the hybrid supports (Table S2), which can be ascribed to the reaction between MAO and FI.¹² The mechanistic process of FI immobilization on POSS/SiO₂ can be deduced as follows: the two Si-OH of POSS react with the Al atoms of MAO layer over the activated silica (when POSS loading ≤ 10 wt%). As a result, there is no extra functional group from POSS to accommodate FI whose immobilization can only take place on the residual MAO which is untethered by POSS. The active sites of FI can therefore be located at distant Al atoms and in the gaps between POSSs. The uniformly isolated active sites of FI are confirmed by the EDX measurements (see Fig. 3c-g), where the Ti elements have been well dispersed and isolated compared with that of the POSS-free support. However, the dispersion of surface Ti atoms becomes worse at 20 wt% of POSS fraction caused by the reaction between the physically adsorbed POSSs and FI.

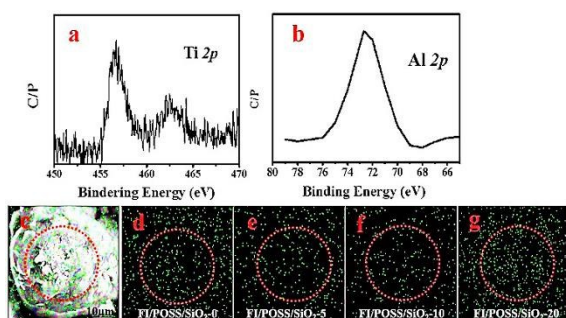


Fig. 3 Characteristics of FI/POSS/SiO₂ catalysts. XPS spectra over the (a) Ti 2*p* region and (b) Al 2*p* region for FI/POSS/SiO₂-

10; (c) Typical reference of EDX; (d-g) Surface distribution of Ti elements measured by EDX.

Table 1 Ethylene polymerization over FI/POSS/SiO₂ catalysts^a

Catalyst	Ti ^b wt%	PE g	Activity ^c	<i>M</i> _w ^d	MWD
FI/POSS/SiO ₂ -0	0.9	8.5	1.8	5.3	2.1
FI/POSS/SiO ₂ -5	1.0	28.6	5.7	4.5	2.4
FI/POSS/SiO ₂ -10	1.0	38.6	7.8	2.0	2.4
FI/POSS/SiO ₂ -20	0.6	7.0	2.3	1.5	1.5
FI-homo	/	42.6	10.6	2.6	1.9

^aPolymerizations: 50 mg of catalyst, 30 mins of reaction, 500 ml of toluene, 10 bar of C₂H₄, 30 °C and 1100 molar ratio of [Al]/[Ti]; ^bmeasured by ICP; ^c10⁵ gPE · mol[Ti]⁻¹ · h⁻¹ · bar⁻¹; ^d10⁶ g · mol⁻¹

The catalytic results of ethylene polymerization are presented in Table 1, where a homogenous system served as comparison purposes. The supported catalyst with no POSS exhibits a lower activity than the homogeneous one. This is due to the bimetallic deactivation resulted from the close distance between each active site.^{8,13} Interestingly, the activity increases obviously when POSS is incorporated. The best specific activity (7.8 × 10⁵ gPE · mol[Ti]⁻¹ · h⁻¹ · bar⁻¹) is achieved with FI/POSS/SiO₂-10 (*i.e.*, with surface saturated POSS), which is four times greater than that over the POSS-free catalyst and directly comparable to that of the homogenous benchmark. The stimulating improvement in activity in this study can be attributed to that the POSSs serve as horizontal spacers between active sites, which enlarge the distance between them and therefore inhibit bimetallic deactivation, consistent with our original hypothesis. We have previously demonstrated chemically bonded FI to POSS only (*i.e.*, no silica) indeed exhibited a detrimental effect on activity due to the increased electronic donation to Ti in Si-O-Ti.^{13,14} The decreased activity of FI/POSS/SiO₂-20 can therefore be linked to the reaction taking place on the FI sites that are bonded to the excessive POSS (Fig. 3g).^{8b,14}

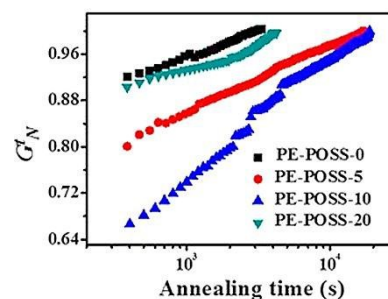


Fig. 4 Dynamic time sweep test (at 180 °C) for the nascent PE with storage modulus (normalized by maximum plateau modulus *G'*_{max}). The synthesized polymer is labelled as PE-POSS-X, where X (= 0, 5, 10 and 20) represents the nominal loading of POSS/SiO₂.

It is noteworthy from the outset that the significantly improvement is not only in the activity of polymerization but also in the product quality. All the synthesized polymer had a molecular weight (M_w) larger than 1 million $\text{g}\cdot\text{mol}^{-1}$, a characteristic of UHMWPE (Table 1). The gel permeation chromatography (GPC) curves of the synthesized UHMWPE are shown in Fig. S6 where the obtained M_w and molecular weight distribution (MWD) of the PE-POSS-0 are increased compared with that of the homogenous one. The confined environment of SiO_2 generates strong transfer resistance to ethylene, where the chain termination can be hindered, increasing the M_w and MWD .^{6,13} However, the incorporation of POSS results in a continuous decrease in M_w and MWD , which may be caused by the increased SSA (Fig. 2a) that enhancing the ethylene diffusion.¹³ Stimulatingly, the synthesized PE shows a weakly entangled state in the FI/POSS/ SiO_2 systems and nascent PE-POSS-10 can approach the most weakly entangled state where the modulus build-up curves shows the lowest starting modulus values and takes the longest time to reach the thermo-dynamically stable melt state (where the modulus is reaching to the maximum, see Fig. 4).^{3,14} The weakly entangled state of PE-POSS-10 can be due to that the steric hindrance generated by the POSS block (Fig. 2c,d), which can enlarge the distance between the growing chains, decreasing accordingly the probability of chain overlap.^{3,4} The PE-POSS-20 becomes more entangled as a result of chain overlapping at the close FI sites (immobilized on physically adsorbed POSS). Moreover, it can be found that the crystallinity and the fraction of monoclinic phase (measured by XRD, See Fig. S7) of PE-POSS-10 can reach the maximum value (80.7% and 15.8%, respectively) because of its less entangled state (See Table S3 and discussion in the ESI). The SEM morphology of the nascent polymers is shown in Fig. S8 where string structure can be noticed particularly in the PE with weakly entangled state.

In summary, POSS-functionalized silica was synthesized and tested as an innovative support of FI for ethylene polymerization. The POSSs were efficiently and evenly bonded to the MAO-activated silica, acting as horizontal spacers, which enlarged the distance between FI and also the growing PE chains. Bimetallic deactivation and chain overlap were thus hindered effectively. An optimal POSS loading (*i.e.*, 10 wt%) was identified for the surface saturation and catalytic performance. The activity of FI/POSS/ SiO_2 -10 was three times higher than that over the FI/ SiO_2 reference and close to that of the homogenous benchmark. The nascent UHMWPE exhibited a weakly entangled state with high crystallinity (80.7%) and a large fraction of monoclinic phase (15.8%). The reported results provide a new strategy for the synthesis of highly effective polymerization catalysts.

This work was supported by the National Natural Science Foundation of China (21206078), Natural Science Foundation of Ningbo (2016A610048) and K.C. Wong Magna Fund in Ningbo University. X.W. also acknowledges support from School of Engineering, the University of Aberdeen.

Notes and references

- 1 W.W. Graessley, *Adv. Polym. Sci.*, 1974, **16**, 1.
- 2 V.M. Litvinov, M.E. Reis, T.W. Baughman, A. Henke and P.P. Matloka, *Macromolecules*, 2013, **46**, 541.
- 3 (a) S. Rastogi, D.R. Lippits, G.W.N. Peters, R. Graf, Y. Yao and H.W. Spiess, *Nature Mater.*, 2005, **4**, 635; (b) S. Ronca, G. Fortem H. Tjaden, Y. Yao and S. Rastogi, *Polymer*, 2012, **53**, 2897; (c) D. Romano, N. Tops, E. Andablo-Reyes, S. Ronca and S. Rastogi, *Macromolecules*, 2014, **47**, 4750; (d) A. Pandey, Y. Champouret and S. Rastogi, *Macromolecules*, 2011, **44**, 4952; (e) Y. Yao, S. Jiang and S. Rastogi, *Macromolecules*, 2014, **47**, 1371.
- 4 A. Osichow, C. Rabe, T. Narayanan, L. Harnau, M. Drechsler, M. Ballauff and S. Mecking, *J. Am. Chem. Soc.*, 2013, **135**, 11645.
- 5 M. Santol, F.A. Gorelli, R. Bini, J. Haines, A. Lee, *Nature Commun.*, 2013, **4**, 1557.
- 6 (a) M. Klapper, D. Joe, S. Nietzel, J.K. Krumpfer and K. Müllen, *Chem. Mater.*, 2014, **26**, 802; (b) S.H. Kim and G.A. Somorjai, *Proc. Natl. Acad. Sci.*, 2006, **103**, 15289; (c) T.F.L. Mckenna, A.D. Martina, G. Weickert and J.B.P. Soares, *Macrom. Reac. Eng.*, 2010, **4**, 40; (d) D.B. Malpass, Introduction to industrial polyethylene: Properties, catalysts, processes, Wiley, Massachusetts, **2010**; (e) E. Groppo, K. Seenivasan, E. Gallo, A. Sommazzi, C. Lamberti and S. Bordiga, *ACS Catal.*, 2015, **5**, 5586-5595.
- 7 D. Gnanasekaran, K. Madhavan and B.S.R. Reddy, *J. Sci. Ind. Res.*, 2009, **68**, 37.
- 8 (a) D. Bianchini, G.B. Galland, J.H.Z. Dos Santos, R.J.J. Williams, D.P. Fasce, I.E. Dell'erba, R. Quijada and M. Perez, *J. Polym. Sci. A-Polym. Chem.*, 2005, **43**, 5465; (b) I. Garcia-Orozco, T. Velilla, G.B. Galland, J.H.Z. Dos Santos, R.J.J. Williams and R. Quijada, *J. Polym. Sci. A-Polym. Chem.*, 2010, **48**, 5938.
- 9 G. Ungar, J. Stejny, A. Keller, I. Bidd and M.C. Whiting, *Science*, 1985, **229**, 386.
- 10 D. Bianchini, J.H.Z. Dos Santos, T. Uozumi and T. Sano, *J. Mol. Catal. A-Chem.*, 2002, **185**, 223.
- 11 (a) M. Choi, F. Kleitz, D. Liu, H. Y. Lee, W. Ahn and R. Ryoo, *J. Am. Chem. Soc.*, 2005, **127**, 1924; (b) H. Li, B. Xu, X. Liu, W. Gao and Y. Mu, *Chem. Commun.*, 2015, **51**, 16703.
- 12 (a) K. Wang, J. Lei and G. Zhou, *RSC Adv.*, 2015, **5**, 70703; (b) M.M.C. Forte, F.V. Cunha and J.H.Z. dos Santos, *J. Mol. Catal. A Chem.*, 2001, **175**, 91; (c) S. Ray, Synthesis, characterization and polymerization of olefins using supported transition metal catalysts. PhD Thesis, University of Pune, **2004**.
- 13 G.G. Hlatky, *Chem. Rev.*, 2000, **100**, 1347.
- 14 (a) W. Li, C. Guan, J. Xu, J. Mu, D. Gong and Z. Chen, *Polymer*, 2014, **55**, 1792; (b) W. Li, T. Chen, C. Guan, D. Gong, J. Mu and Z. Chen, *Ind. Eng. Chem. Res.*, 2015, **54**, 1478.